Heart Rate Estimation From PPG Signals Corrupted By Intense Motion Artifacts With Dynamic Channel Selection And Least Mean Kurtosis Adaptive Denoising

M.K. Hasan, Ashraful Islam, Md. Tauhiduzzaman Khan

***Abstract*—Estimating heart rate from Photoplethysmographic (PPG) signal during intense physical activities is a challenging and difficult task, since the signal is heavily corrupted by motion artifact (MA) in this case. With the advent of wearable devices, development of HR estimation framework that would work even when the subject is running or walking is commercially valuable. In this paper, we propose a novel heart rate estimation framework named CHASER for MA corrupted multichannel PPG signal. In our framework, we first select single channel by dynamic channel selection algorithm. We then apply two stage denoising techniques called LMK-RLS algorithm and decomposition based denoisong with singular spectrum analysis. We then apply our tracking algorithm to select the correct heart rate peak frequency. Finally, we do fine tuning and check the validity of the estimated HR with sudden movement detection algorithm. Using this framework, the average absolute error of 0.76 and standard deviation of 1.13 are reported for 12 subjects performing physical activities. Our performance shows great improvement over existing algorithms in this field like TROIKA, JOSS, MURAD, Khan *et al.*. This framework has a great value in wearable devices even when severe MA is present.**

I. Introduction

Photoplethysmography (PPG) has become a very popular and low-cost technique to measure heart rate (HR). HR estimation was previously done using electrocardiography (ECG) signal. Though ECG gives very good HR estimation, its costly implementation and hardware complexity have limited its usability. The non-invasive and simple nature of PPG technology have motivated its presence in wearable devices. Besides HR estimation, PPG signals can be used for measuring blood oxygen level, systolic blood pressure [1], vascular assessment, respiratory rate [2], [3]. PPG signal is obtained by pulse oximator implemented in small wearable devices to be put on earlobes or fingertips or wrists. Pulse oximator consists of one LED and one photo-detector. The LED emits light which travels through biological tissues. Light is absorbed by bones, skin pigments and both venous and arterial blood. Since light is more strongly absorbed by blood than the surrounding tissues, the changes in blood flow can be detected by photo-detector as changes in the intensity of light. As amount of blood varies with the changes cardiac rhythm, light intensity also varies with cardiac cycle. Thus PPG waveform can be used to measure heart rate. However, the main disadvantage of using PPG signal in HR measurement is that PPG signals are very much vulnerable to motion artifacts (MA), specially during HR monitoring in fitness, interference of MA in PPG signal is unavoidable. Presence of MA has made it difficult to estimate HR as MA peak and HR peak can coincide to very close proximity. Also, intense MA can suppress HR peak and makes it difficult to estimate HR. So, it is a challenging task to measure HR from PPG signal corrupted by intense motion artifacts.

Severel methods have been proposed to overcome the problem of MA and measure heart rate. Ram *et al.* [4] applied adaptive noise cancellation (ANC) technique to remove MA. Though this method has the capability of continuous processing during time-varying condition, it is highly sensitive to the choice of reference signal, which is very difficult to obtain when the subject is in intense physical activity. Empirical mode decomposition (EMD) has been used for artifact reduction in [5]. But this technique considers all the modes instead of extracting the modes that are suitable for HR estimation. EMD has been used in [10], [11] and [12]. Peng *et al.* [15] applied independent component analysis (ICA) and least mean square (LMS) adaptive filters to estimate HR. Moreover, Krishnan *et al.* [9] propose a frequency domain ICA technique for artifact removing. However, ICA assumes that MA and HR are statistically independent. Though this assumption holds to be partially true for limited motion, in intense motion high correlation is found between MA and HR. Thus MA reduction is not satisfactory in this case.

Often three axes accelerometer data is used to model the motion artifact present in PPG data [6]. With the advent of wearable gadgets, this method has become popular and has been widely used recently. Kim *et al.* utilized z-axis accelerometer data as reference noise signal [7]. Poh *et al.* adopted a predefined time-sharing approach for the 3 axis accelerometer data, but for a certain instant only single axis data were used [8]. Kalman filtering has also been used to remove MA [13]. But Kalman filtering is not good for real-time heart rate monitoring, it requires more than double of computational time than adaptive filtering [14]. So, its application is limited in wearable devices. In [16], [17] and [18] Hr estimation techniques reported improved result. But, all of these techniques consider fingertip-type PPG where MA is less intense compared to wrist-type PPG.

Recently, TROIKA [20] , JOSS [21], Khan *at el.* [19] and MURAD [22] have been proposed for HR estimation corrupted by intense MA. TROIKA framework consists of three stage

general framework and incorporates singal decomposition stage to remove MA, but this procedure can not remove all MA. JOSS framework is an improvement over TROIKA framework that incorporates signal sparsification technique, though it is still heavily dependent on tracking mechanism. Recently, dual channel PPG signals are being used in HR estimation. Implementing dual channel PPG in wearable devices does not cost much and it can be used in robust HR estimation. Khan *et al.* applied recursive least square (RLS) adaptive filter and EMD to remove MA. MURAD framework utilized four reference signal, three axes accelerometer data and difference between two PPG channels, and applied applied adaptive noise cancellation algorithm. Most of the cases, one PPG channel is better for estimation. None of the methods addressed the challenge of selecting better PPG channel dynamically in multichannel PPG signals. Also, those methods suffer greatly when MA peak and HR peak frequency coincide closely.

In this paper, we propose a novel framework termed CHASER to remove MA from PPG signals and estimate HR correctly. It consists dynamic CHAnnel SElection with least mean kurtosis Recursive least square adaptive algorithm. First, we select the correct channel dynamically. To do this, we estimate power spectral density (PSD) of the PPG channels from Burg's method. As Burg method is a parametric spectral estimation and has high resolution, it is suitable for short PPG data segment. Then we measure kurtosis of the PSD within a certain window. The channel having higher kurtosis value selected as better channel. After that we apply two stage denoising technique–filter based denoising and decomposition based denoising–to remove MA. Filter based denoising is performed with RLS algorithm. As traditional RLS algorithm often fails to remove MA from PPG signals, even sometimes distorts the signal by removing HR information containing part, we add a kurtosis constraint in the RLS cost function and calculate the update equation. We term this algorithm as least mean kurtosis RLS (LMK-RLS) algorithm. We also apply decomposition based denoising with singular spectrum analysis (SSA). Both of the denoising methods are performed in a parallel manner. We then apply some heuristic peak verification techniques and our tracking algorithm to estimate HR from denoised signals.

The rest of the paper is organized as follows: Section II discusses problem insights and motivations. Section III presents the technical details of our proposed methods. Section IV illustrates experimental results and comparison with other frameworks. The paper is concluded in Section V with remarks.

II. Problem Insights and Motivitation

Estimating HR from MA corrupted PPG signal is a challenging task. Without proper denoising method, robust and accurate HR monitoring system can not be implemented. One problem relating to intense movement while measuring measuring PPG signal is that the space between wrist or fingertip and oximeter changes. So, the light intensity changes which affects intensity of PPG signal. This variation can be tracked, as it has correlation with the frequency of movement.

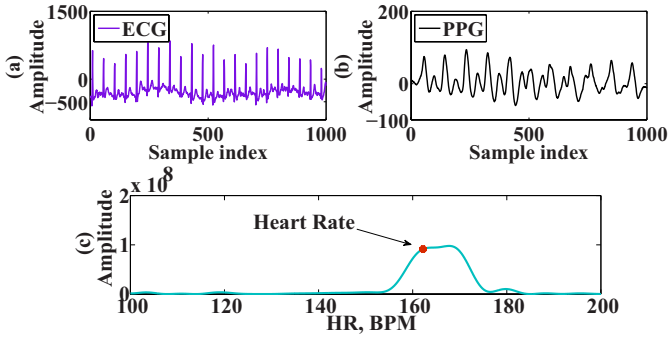

Fig. 1: A segment of (a) the ECG signal and (b) the corresponding PPG signal in time domain. (c) Periodogram of the PPG signal shows that the MA peak and the HR peak are almost indistinguishable from each other.

However, sometimes the distance might be so far apart that the light intensity becomes too law and HR peak might be totally lost. This situation has to be handled, otherwise wrong estimation might be resulted. Moreover, intense motion like boxing, jumping etc may cause so much acceleration in the blood that highest peak might not correspond to actual HR, rather the acceleration frequency [24].

One of the major problems is that the MA peak and HR peak might be so close that they may get indistinguishable. Fig. 1 illustrates this situation. This is the situation when major denoising algorithm fails. Though LMS and RLS adaptive algorithm have been utilized to remove MA by using accelerometer data as reference signal, these methods often corrupts the actual HR information bearing signal. Fig. 2 illustrates this situation when RLS filtering distorts the raw PPG signal. One of the major novel contributions in our proposed algorithm is to address this situation by incorporating a constraint function in the RLS cost function to preserve the HR information bearing signal and modify the RLS algorithm accordingly. To find out the constraint, we exploit the characteristic that is preserved in a clean PPG segment, which is kurtosis. Fig. 2a shows that each period of a clean PPG segment is tailed shaped. Kurtosis is a statistical characteristics that denotes the taileness of a distribution function. We use kurtosis based constraint function in RLS cost function so that this tailedness property is present after RLS filtering is applied on raw PPG signal.

Sometimes, intense motion like boxing, jumping etc may cause so much acceleration in the blood at the arteries, that even correct intensity might not correspond to actual HR [24].

Since actual HRs do not show sudden discontinuity, this provides an important a priori information for HR estimation. But this also can destroy the robustness of the estimation. For example, if in one segment MA peak is mistakenly calculated as HR peak, this subsequently increase error in the later segments even if the original HR peaks get stronger in later time.

III. Methods

In this section, we propose our framework to overcome the aforementioned problem of MA reduction and HR estimation.

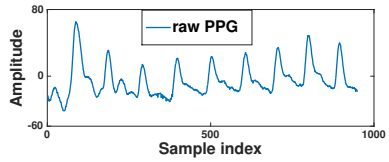

(a)

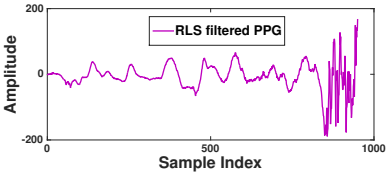

(b)

Fig. 2: A segment of (a) raw PPG signal and (b) PPG signal after RLS filtering is applied. It shows that RLS filtering distorts the PPG segment.

A. Data Description

We run our algorithm on the same datasets used in [20] and [21]. This is the dataset provided by the IEEE Signal Processing Cup, 2015 [23], titled Heart Rate Monitoring During Physical Exercise Using Wrist-Type Photoplethysmographic (PPG) Signals, where 12 healthy male subjects (age ranging from 18 to 35) ran on a tread mill with speeds reaching upto 15 km/hr. The data consist of two- channel PPG signals, three-axis acceleration signals, and one- channel ECG signal simultaneously recorded from subjects. For each subject, the PPG signals is recorded from wrist by two pulse oximeters with identical green LEDs (wavelength: 515nm). Their distance was 2 cm. The acceleration signal is also recorded from wrist by a three-axis accelerometer. Both the pulse oximeter and the accelerometer were embedded in a wristband. The ECG signal is recorded simultaneously from the chest of each subject using wet ECG sensors. All signals were sampled at 125 Hz. The given data set is divided into training and testing ones. The training set consists of data recordings from 12 male subjects. During data recording, the subjects walked or ran on a treadmill with varying speed ranging from 6-8 km/hour to 12-15 km/hour. The 10 testing datasets were recorded from 8 subjects aging from 19 to 58. One of them even had abnormal heart rhythm and blood pressure too. Moreover, the subjects are instructed to perform more complicated and intense physical exercises such as shake hands, stretch, push, running, jump, push-up, boxing, etc and even swimming and weight-lifting in some extreme cases.

B. Signal Modeling

We are given two channels of raw PPG segments $y_{i,\text{raw}}(n)$ $(i = 1, 2)$ and the corresponding raw acceleration segments $a_{\gamma,\text{raw}}(n)$ ($\gamma = x, y$ and z) at a sampling frequency F_s. We also calculate $y_{\text{avg}}(n)$ and $a_{\text{xyz}}(n)$ as follows :

$$y_{\text{avg}}(n) = \frac{1}{2}[y_{1,\text{raw}}(n) + y_{2,\text{raw}}(n)]$$

$$a^2_{\text{xyz}}(n) = a^2_{x,\text{raw}}(n) + a^2_{y,\text{raw}} + a^2_{z,\text{raw}}(n)$$

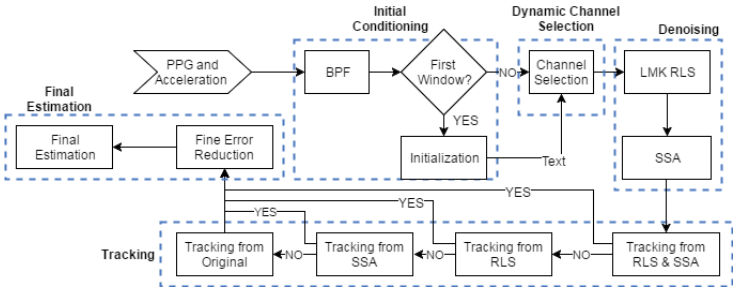

Fig. 3: Block diagram of CHASER framework

We divide the whole PPG data into segment of length L where

$$L = 1000 * \frac{F_s}{125} \tag{1}$$

We can model the MA corrupted raw PPG segments $y_{i,\text{raw}}(n)$ $(i = 1, 2)$ by

$$y_{i,\text{raw}}(n) = d_i(n) + v_i(n); \quad n = 0, 1, \ldots, M-1$$

where $d_i(n)$ is the desired clean PPG signal and $v_i(n)$ is the signal due to motion artfact. We assume $v_i(n)$ has high correlation with $a_{\gamma,\text{raw}}(n)$, so it can be removed by properly utilizing the accelerometer signal.

First we normalize $y_{i,\text{raw}}(n)$ $(i = 1, 2)$ and $a_{\gamma,\text{raw}}(n)$ ($\gamma = x, y$ and z) by dividing each signal with the RMS mean of the whole data. Then we perform smoothing operation on PPG data and acceleration data by bandpass filtering with lower and upper passband cut-off of 40 BPM and 300 BPM. After that we perform RLS algorithm on the first segment of the data. To measure a crude frequency estimate of the initial segment, we perform our initialization algorithm on the filtered signal. Then we select the proper PPG channel using our channel selection algorithm, and apply least mean kurtosis RLS algorithm on the selected channel. Then we use spectrum estimation and peak tracking techniques to select estimated heart rate. Finally, we use fine error reduction technique to get the actual HR. We describe the proposed method in details as follows :

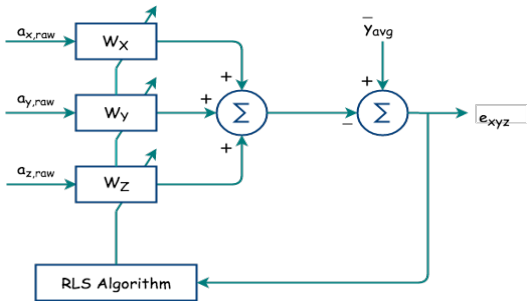

Fig. 4: RLS block for initial window

C. Initial Measurement

Here we describe our initial method to measure a crude estimate of the HR from first data segment. In Fig. 4 we describe our noise reduction method using RLS. We use filtered average PPG data segment $\bar{y}_{\text{avg}}(n)$ as desired signal

and three acceleration data segment $a_{\gamma,\text{raw}}(n)$ ($\gamma = x, y$ and z). Each of the segments has length of L found from 1. There are several methods to combine the acceleration data. In [19], three separate RLS blocks were used to denoise initial segment, that attempts to remove noisy part due to $a_x(n)$, $a_y(n)$ and $a_z(n)$ separately. We see that this method fails to give correct initial estimation for all subjects and it is also time consuming to use three separate RLS blocks. Moreover, The estimation using $a_x^2 + a_y^2 + a_z^2$ fails to give correct prediction too. In our approach, we calculate the error signal of RLS filter $e_{\text{xyz}}(n)$ which acts as denoised PPG signal as follows :

$$\begin{aligned} e_{\text{xyz}}(n) = \bar{y}_{\text{avg}}(n) - a_{x,\text{raw}}(n) * w_x(n) - a_{y,\text{raw}}(n) * w_y(n) \\ - a_{z,\text{raw}}(n) * w_z(n) \\ = \bar{y}_{\text{avg}}(n) - \sum_{\gamma=x,y,z} \sum_{k=1}^{p-1} w_\gamma(k) a_{\gamma,\text{raw}}(n-k) \end{aligned}$$

where p is the RLS fiter length, which is 10 in our experiment and $w_x(n)$,$w_y(n)$ and $w_z(n)$ are the RLS filter coefficients that are updated adaptively by minimizing error function

$$J_e(n) = \frac{1}{2} \sum_{i=0}^{n} \lambda^{n-i} |e(i)|^2 \tag{2}$$

The error signal $e_{\text{xyz}}(n)$ found in this way is assumed not to have motion artifact contribution correlated to $a_x(n)$, $a_y(n)$ and $a_z(n)$. We rename $e_{\text{xyz}}(n)$ as denoised signal $r(n)$. After denoising the initial segment we take calculate f_{prev} as follows:

- At first, dominant frequency peaks from $r(n)$ is put into S_{rls}. We use Fourier based spectral analysis for determining dominant peaks. If S_{rls} contains the location of only the maximum peak, then we assign that to f_{prev}.
- If S_{rls} contains more the one peak, then there are multiple strong peaks present. Therefore, we look for their second harmonics in S_{rls} and build a new set $H_{\text{rls}} \subset S_{\text{rls}}$ so that for each $x \in H_{\text{rls}}$ then there exists a $y \in S_{\text{rls}}$ such that $|2x - y| < 5$ BPM. If H_{rls} is not empty, then the strongest peak is assigned to f_{prev}.
- If H_{rls} is empty, then we first construct a set $S_{\text{a, 0.8}}$ by taking all the dominant peaks (80% of the maximum peak) from the acceleration signals $a_\gamma(n)$, and then cross out all the peaks in S_{rls} which are close to the acceleration peaks stored in $S_{\text{a, 0.8}}$ within a 5 BPM range by forming $S = S_{\text{rls}} \setminus^5 S_{\text{a, 0.8}}$. Here for notational convenience, we define $A \setminus^\delta B = \{x \in A : |x - y| > \delta \text{ BPM}, \ \forall y \in B\}$. Next if S is not empty the strongest peak in S is assigned to f_{prev}.
- If f_{prev} is still not assigned (which is a rare case), then we assign its value to the strongest peak's location in S_{rls}. As we shall see later, even if f_{prev} is erroneously initialized, our main algorithm is designed in such a way that it can correct for it later and come back on track.

D. Dynamic Channel Selection

One of the major tasks in our algorithm is to determine clean PPG channel from the two channels. We chose our selection algorithm using Burg parametric estimation and kurtosis of signal spectrum. To select proper channel, first we have to measure Power spectral Density(PSD) of the channel segments. We calculate PSD using Burg method, instead of more conventional periodogram method. Burge method produces very high resolution estimates, like all auto-regressive methods, because it uses linear prediction to extrapolate the signal outside of its known data record. This effectively removes all sidelobe phenomena. It is superior to the other parametric methods like Yule-Walker method for short data records. PSD from Burge method is also suitable for kurtosis calculation. We first determine the Auto-regressive power spectral density of each channel $y_{i,\text{raw}}(n)(i = 1, 2)$ using Burg's method. The burg power spectrum of $y_{i,\text{raw}}(n)$ is $P_{burg,i}(f)$. We select a subset of $P_{burg,i}(f)$, where $f_{\text{prev}} - 15BPM < f < f_{\text{prev}} + 15BPM$, which is denoted as $P_{subset,i}(f)$. Then we calculate the kurtosis of each set by using :

$$k_i = \frac{\frac{1}{n} \sum\limits_{f_{\text{prev}}-15<f<f_{\text{prev}}+15} (P_{subset,i}(f) - \overline{P_{subset,i}(f)})^4}{(\frac{1}{n} \sum\limits_{f_{\text{prev}}-15<f<f_{\text{prev}}+15} (P_{subset,i}(f) - \overline{P_{subset,i}(f)}))^2}$$

where i = 1,2. The correct channel index c is selected from :

$$c = \arg\max_i k_i$$

The selected channel thus found is $y_c(n)$.

E. MA Reduction Using Least Mean Kurtosis RLS Algorithm

Now, we remove motion artifact from noisy PPG channel. This can be done by implementing traditional RLS algorithm. We first define,

$$e(i) = y_c(i) - \sum_{k=1}^{p-1} w(k) a_{\text{xyz}}(i-k) = y_c(i) - \mathbf{w}^T \mathbf{a}_{\text{xyz}}(i) \tag{3}$$

where

$$\mathbf{w} = \begin{bmatrix} w(0) & w(1) & w(2) & \cdots & w(p-1) \end{bmatrix}^T$$

and

$$\mathbf{a}_{\text{xyz}}(i) = \begin{bmatrix} a_{\text{xyz}}(i) & a_{\text{xyz}}(i-1) & \cdots & a_{\text{xyz}}(i-p+1) \end{bmatrix}^T$$

Using the RLS cost function as of (2), denoising can be implemented. But, in Fig 2b, we see that traditional RLS sometimes distorts actual PPG data. If there is high correlation between motion artifact and actual PPG data containing HR information, specially when frequency of HR and frequency of hand movement coincide,extracting clean PPG using cost function of 2 can remove actual HR containing signal. We add a constraint function in RLS cost function that can preserves clean PPG characteristics and at the same time removes motion artifact. New RLS cost function is given as :

$$J(n) = J_e(n) + \alpha J_s(n) \tag{4}$$

where

$$J_e(n) = \frac{1}{2} \sum_{i=0}^{n} \lambda^{n-i} |e(i)|^2 \tag{5}$$

and $J_s(n)$ is the negated kurtosis

$$J_s(n) = 3E^2[e(n)]^2 - E[e^4(n)] \quad (6)$$

Now, Taking gradient of 4 with respect to $\mathbf{w}$ we get,

$$\begin{aligned}
\nabla J(n) &= \frac{1}{2}\sum_{i=0}^{n}\lambda_{n-i}\nabla|e(i)|^2 + \nabla J_s(n) \\
&= \frac{1}{2}\sum_{i=0}^{n}\lambda_{n-i}\frac{d}{d\mathbf{w}}|e(i)|^2 + \nabla J_s(n) \\
&= \frac{1}{2}\sum_{i=0}^{n}\lambda_{n-i}2e(i)\frac{d}{d\mathbf{w}}e(i) + \nabla J_s(n) \\
&= \sum_{i=0}^{n}\lambda_{n-i}e(i)\frac{d}{d\mathbf{w}}e(i) + \nabla J_s(n) \\
&= -\sum_{i=0}^{n}\lambda_{n-i}e(i)\mathbf{a}_{\text{xyz}}(i)_T + \nabla J_s(n) \\
&= -\sum_{i=0}^{n}\lambda_{n-i}\ [y_c(i) - \mathbf{w}^T\mathbf{a}_{\text{xyz}}(i)]\ \mathbf{a}_{\text{xyz}}(i)^T \\
&\quad + \nabla J_s(n) \\
&= -\sum_{i=0}^{n}\lambda_{n-i}\ y_c(i)\ \mathbf{a}_{\text{xyz}}(i)^T \\
&\quad + \sum_{i=0}^{n}\lambda_{n-i}\ \mathbf{w}^T\mathbf{a}_{\text{xyz}}(i)\ \mathbf{a}_{\text{xyz}}(i)^T + \nabla J_s(n) \\
&= -\mathbf{\Psi}(n) + \mathbf{\Phi}(n)\mathbf{w} + \nabla J_s(n)
\end{aligned}$$

where,

$$\mathbf{\Psi}(n) = \sum_{i=0}^{n}\lambda_{n-i}\ y_c(i)\ \mathbf{a}_{\text{xyz}}(i)^T$$

$$\mathbf{\Phi}(n) = \sum_{i=0}^{n}\lambda_{n-i}\ \mathbf{w}^T\mathbf{a}_{\text{xyz}}(i)\ \mathbf{a}_{\text{xyz}}(i)^T$$

To minimize $J(n)$ we set $\nabla J(n) = 0$. So,

$$\mathbf{\Phi}(n)\mathbf{w} = \mathbf{\Psi}(n) - \nabla J_s(n) = \mathbf{\Gamma}(n)$$

Now,

$$\mathbf{\Phi}(n) = \lambda\mathbf{\Phi}(n-1) + y_c(n)\mathbf{a}_{\text{xyz}}(n)$$

$$\mathbf{\Psi}(n) = \lambda\mathbf{\Psi}(n-1) + \mathbf{a}_{\text{xyz}}(n)\ \mathbf{a}_{\text{xyz}}(n)^T$$

So,

$$\begin{aligned}
\mathbf{\Gamma}(n) &= \mathbf{\Psi}(n) - \nabla J_s(n) \\
&= \lambda\mathbf{\Phi}(n-1) + y_c(n)\mathbf{a}_{\text{xyz}}(n) - \nabla J_s(n) \\
&= \lambda\ [\mathbf{\Phi}(n-1) - \nabla J_s(n)\ ] + y_c(n)\mathbf{a}_{\text{xyz}}(n) - \\
&\quad (1-\lambda)\nabla J_s(n) \\
&= \lambda\mathbf{\Gamma}(n-1) + y_c(n)\mathbf{a}_{\text{xyz}}(n) - (1-\lambda)\nabla J_s(n)
\end{aligned}$$

Here, we are assuming $\nabla J_s(n) \simeq \nabla J_s(n-1)$. By using matrix inversion lemma, we can show that ,

$$\mathbf{P}(n) = \frac{1}{\lambda}\ [\mathbf{P}(n-1) - \mathbf{k}_n\ \mathbf{a}_{\text{xyz}}(n)^T\mathbf{P}(n-1)\ ]$$

where,

$$\mathbf{P}(n) = \Phi^{-1}(n)$$

$$\mathbf{k}_n = \frac{\mathbf{P}(n-1)\mathbf{a}_{\text{xyz}}(n)}{\lambda + \mathbf{a}_{\text{xyz}}(n)^T\mathbf{P}(n-1)\mathbf{a}_{\text{xyz}}(n)}$$

$$P(n)\mathbf{a}_{\text{xyz}}(n) = \mathbf{k}_n$$

Now,

$$\begin{aligned}
\mathbf{w}_n &= \mathbf{P}(n)\mathbf{\Gamma}(n) \\
&= \mathbf{P}(n)\ [\lambda\mathbf{\Gamma}(n-1) + y_c(n)\mathbf{a}_{\text{xyz}}(n) - (1-\lambda)\nabla J_s(n)\ ] \\
&= \lambda\frac{1}{\lambda}[\mathbf{P}(n-1) - \mathbf{k}_n\ \mathbf{a}_{\text{xyz}}(n)^T P(n-1)]\mathbf{\Gamma}(n) \\
&\quad + y_c(n)\mathbf{P}(n)\mathbf{a}_{\text{xyz}}(n) - (1-\lambda)\mathbf{P}(n)\nabla J_s(n) \\
&= \mathbf{w}_{n-1} + \mathbf{k}_n[y_c(n) - \mathbf{a}_{\text{xyz}}(n)^T\mathbf{P}(n-1)\mathbf{\Gamma}(n)] \\
&\quad -(1-\lambda)\mathbf{P}(n)\nabla J_s(n) \\
&= \mathbf{w}_{n-1} + \mathbf{k}_n.\mathbf{a}_{\text{xyz}}(n)^T\mathbf{w}_n - (1-\lambda)\mathbf{P}(n)\nabla J_s(n) \\
&= \mathbf{w}_{n-1} + \mathbf{k}_n[y_c(n) - \mathbf{w}_n{}^T\mathbf{a}_{\text{xyz}}(n)] \\
&\quad -(1-\lambda)\mathbf{P}(n)\nabla J_s(n) \\
&= \mathbf{w}_{n-1} + \mathbf{k}_n[y_c(n) - \mathbf{a}_{\text{xyz}}(n)^T\mathbf{a}_{\text{xyz}}(n)] \\
&\quad -(1-\lambda)\mathbf{P}(n)\nabla J_s(n) \\
&= \mathbf{w}_{n-1} + \mathbf{k}_n e(n) - (1-\lambda)\mathbf{P}(n)\nabla J_s(n)
\end{aligned}$$

Taking gradient of (6) with respect to $\mathbf{w}_n$

$$\nabla J_s(n) = 4[3G(n) - e^2(n)]e(n)\mathbf{a}_{\text{xyz}}(n)$$

where

$$G(n) = \beta G(n-1) + (1-\beta)e^2(n)$$

In our algorithm, we set RLS filter length p to 10, β to 0.01 and λ to 0.9958. We apply least mean kurtosis RLS filtering in both the selected PPG channel $y_c(n)$ and average PPG channel $y_{\text{avg}}(n)$, and we get filtered signal $y_{f,\text{c}}(n)$ and $y_{\text{f,avg}}(n)$ respectively.

F. Spectrum Estimation & Peak Detection from RLS

Here, we calculate signal peak frequencies using Fourier based method from two estimation. We first put dominant peaks from $y_{f,\text{f,c}}(n)$ and $y_{\text{f,avg}}(n)$ (40% of the maximum) into S_{rls}. S_{rls} may have several closely spaced frequencies, as it contains frequencies from two channels. In this case, we applied clustering in S_{rls}. The clustering is done as followes: we divide S_{rls} intro several subsets $H_i(i = 1, 2, 3, ...)$ such that for each $f_k \in H_i$ and $f_l \in H_i$, $|f_k - f_l| < 5$. We then take mean of each H_i and put the mean values into $S_{\text{clustered}}$.

G. Denoising based on SSA

We apply another denoising technique based on singular spectrum analysis (SSA). SSA is a decomposition based denoising and it is completely a time series analysis. It is performed as follows:

For PPG data segment $y_\gamma(n)(\gamma = 1, 2)$, where n varies from 1 to segment length L, we first form a Toeplitz matrix(each diagonal has a uniform value) with lag size M by

$$c_{ij} = \frac{1}{L - |i-j|}\ \sum_{t=1}^{L-|i-j|}\ y_\gamma(t)y_\gamma(t+|i-j|) \quad 0 \le i, j \le M-1 \quad (7)$$

The eigenvalues λ_k and eigenvectors E_j^k of this matrix are calculated and sorted in descending order of λ_k, where j and k varies from 1 to M. The kth principle component is calculated by

$$a_i^k = \sum_{j=1}^{M} y_\gamma(i+j)E_j^k \quad 0 \le i \le L-M \tag{8}$$

Now, the kth reconstructed component (RC) series is given by

$$y_{\gamma,i}^k = \frac{1}{M}\sum a_{i-j}^k E_j^k \quad M \le i \le L-M+1 \tag{9}$$

The fraction of the total variance of the original time series $y_\gamma(n)$ contained in kth RC is λ_k. Here, RCs are ordered by decreasing information about the original time series. Most of the variance is contained in the first several RCs. In our setup, we set M to 400 and we reconstruct the signal by adding first 10 RC components. We calculate reconstructed signal from both $y_{f,\text{c}}(n)$ and $y_{\text{f,avg}}(n)$, and calculate peak frequencies (60% of the maximum). After clustering following previous method of peak detection from RLS, we get $S_{\text{clustered,SSA}}$.

We then construct a set S_{freq} such that for each $x \in S_{freq}$ we have $x \in S_{\text{clustered}}$ and $x \in S_{\text{clustered,SSA}}$. We also put dominant peaks (80% of the maximum) from $a_{xyz}(n)$ into S_{acc}.

H. Peak Tracking

Tracking from RLS & SSA :

- If $S_{\text{clustered}}$ contains only one peak f_{freq} and $|f_{freq} - f_{prev}| < 14$ then we assign $f = f_{freq}$. Otherwise, we construct $S_{\text{clustered}} \setminus^3 S_{\text{acc}}$. If this set is non-empty, we construct $S_{peak} = \{x \in S_{\text{clustered}} \setminus^3 S_{\text{acc}} : |x - f_{prev}| < 6\}$. We assign $f_{prev} = mean(S_{peak})$.
- If the previous step fails to give frequency estimate, then we calculate peak frequencies (50 % of the maximum) of y_{avg} and put them into S_{avg}. Then we proceed the same way as the previous tracking.
- If the tracking from both of the above steps fails to give crude estimate, then we use $S_{\text{clustered,SSA}}$, and proceed the same way as before.

Tracking from the original signal :

If the above steps fail to provide with the crude estimate f, then we consider all the peak locations attainable from the periodograms of $y_i(n)$ and array them together in a set S_{org}. We also construct another set $S_{\text{a,0}}$ by taking all the peaks from $a_\gamma(n)$. Next we take the peak $f_{\text{org}} \in S_{\text{org}}$ which is closest to f_{prev} and also $|f_{\text{org}} - f_{\text{prev}}| \le 5$ BPM. Then if $f_{\text{org}} \in S_{\text{org}} \setminus^3 S_{\text{a, 0}}$ then we assign $f = f_{\text{org}}$. If no peak found in this way, then we conclude that the PPG segment so much corrupted with MA that HR information is totally lost in the segment. Therefore, we assign $f = f_{\text{prev}}$.

I. Fine Error Reduction

This is the final step of our algorithm where we attempt to obtain a fine estimate f_{est} from the crude estimate f by working with the raw PPG data. To do so we construct a set S_{raw} by taking all the peak locations attainable from the periodograms of $y_{i,\text{raw}}$. Then we look for the peak $f_{\text{raw}} \in S_{\text{raw}}$ which is closest to f and also $|f_{\text{raw}} - f| \le \Delta_{\text{fine}}$ with Δ_{fine} around $3 \sim 4$ BPM. If such a peak is found then we assign our fine estimate $f_{\text{est}} = f_{\text{raw}}$. Otherwise, we consider our crude estimate as the final estimate $f_{\text{est}} = f$.

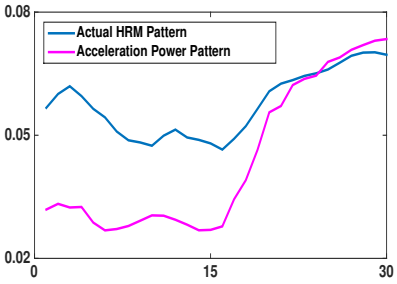

Fig. 5: Pattern between actual HR and acceleration power

J. Sudden Movement Detection

There is a correlation between heart rate and movement. We have seen that sudden movement increases the heart rate. We can explore this fact by observing the track of actual HR and movement power. Movement power can be detected from power of acceleration data. We calculate the power of the acceleration data as follows :

$$P_{acc} = \frac{1}{L}\sum_{i=1}^{L}\sum_{\gamma=x,y,z} a_{\gamma,\text{raw}}^2(i)$$

From Fig.2 , we see that actual HR follows movement power. Initially, in our data set there is no movement as the subject is assumed to be on rest. When the subject starts to move, his heart rate increases gradually. This gradual increse can be apparent from Fig.4. By observing this phenomena in 12 subjects, we determine a threshold of sudden movement. In our data-set, if $P_{acc} > 1$, then we decide that sudden movement occurs. In this case, we have a prior information that heart rate must increase gradually. We show that this prior information is helpful in many estimation. Therefore, we consider movement detection in the final estimation. If we find sudden movement occurs, then we check if $f_{\text{est}} > f_{\text{prev}}$. If this is not the case, then we set $f_{\text{est}} = f_{\text{prev}} + 3$. Also in this step we assign $f_{\text{prev}} = f_{\text{est}}$ for the next time window.

IV. Result Analysis

A. Performance Measurement

The primary performance measurement index to ealuate the accuracy of our method is average absolute error (AAE) defined as,

$$AAE = \frac{1}{N}\sum_{i=1}^{N} |BPM_{\text{est}}(i) - BPM_{\text{true}}(i)| \tag{10}$$

where $BPM_{\text{true}}(i)$ is the ground truth of HR at i th window and $BPM_{\text{est}}(i)$ is the estimated HR of that window.

Moreover, Bland-Altman plot was another evaluation index which shows the difference between each estimate and the

TABLE I: Performance comparision of different algorithms using average absolute errors for the 12 datasets.

	Subj 1	Subj 2	Subj 3	Subj 4	Subj 5	Subj 6	Subj 7	Subj 8	Subj 9	Subj 10	Subj 11	Subj 12	Mean ± SD
CHASER	1.08	0.74	0.65	0.92	0.48	0.85	0.59	0.50	0.32	1.37	0.84	0.78	0.76 ± 1.13
JOSS [21]	1.33	1.75	1.47	1.48	0.69	1.32	0.71	0.56	0.49	3.81	0.78	1.04	1.28 ± 2.61
TROIKA [20]	3.05	3.31	1.49	2.03	1.46	2.35	1.76	1.43	1.28	5.08	1.80	3.02	2.34 ± 2.86
MURAD [22]	1.17	0.93	0.7	0.82	0.88	0.97	0.67	0.74	0.49	2.69	0.81	0.77	0.97 ± 1.82
Khan *et al.* [19]	1.64	0.81	0.57	1.44	0.77	1.06	0.63	0.47	0.52	2.94	1.05	0.91	1.07 ± 2.17

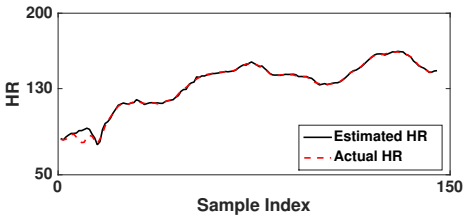

(a)

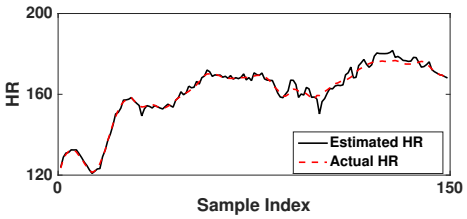

(b)

Fig. 6: HR estimation on two dataset (a) Subject 4 (B) Subject 10

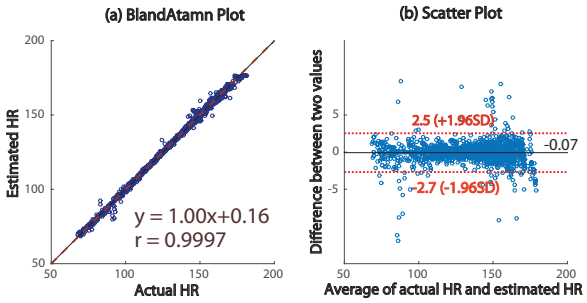

Fig. 7: Bland Atman and Scatter plot

associated ground-truth HR against their average. In this analysis we also calculated Limit of Agreement (LOA), which is defined as $[\mu\ \ 1.96\sigma\ ,\ \mu + 1.96\sigma]$, where μ is the mean of the error difference and σ is the corresponding standard deviation. Pearson correlation coefficent was also used as an evaluation index.

B. Result

We first represent our estimation result on two random dataset - subject 4 and subject 10. These two dataset are highly corrupted with MA. We can see in 6 that our estimation algorithm can track actual HR quite perfectly.

In Table I, we present the value of AAE for 12 subjects. Also, the result obtained for TROIKA, JOSS, MURAD, Khan *et al.* are also presented for comparison. It is seen that the performance of CHASER framework is better than all other frameworks in the literature. Average absolute error is calculated to be 0.76, which is better than the previous best estimation 0.97 by MURAD. The standard deviation is 1.13 which is also better than all other estimates.

The Bland-Altman plot between ground-truth and estimates is given in Fig. 7a. In this case, the Limit of Agreement (LOA) was [-2.7,2.5] BPM and 96.833% of all differences were inside this range. In JOSS, the LOA was [-5.94, 5.41] BPM. For TROIKA, it was [-7.26, 4.79] BPM and for MURAD, it was [-3.57,3.61] BPM. Clearly, Bland-Atman analysis shows greater inmprovement in our framework.

Figure 7b shows the Scatter Plot between the ground-truth heart rate values and the associated estimates over the 12 datasets. It shows that the fitted line was Y = X + 0.16, where X denotes the ground-truth heart rate value, and Y indicates the associated estimate. The Pearson coefficient in our framework was 0.9997. On the other hand, this metric for TROIKA was 0.992, for JOSS it was found to be 0.993, for MURAD it was 0.9972 and for Khan *et al.* it was 0.996. Pearson coefficient is also improved in our methodology.

V. Conclusion

This paper has proposed a novel framework for heart rate estimation in intense physical activities. We develop proper channel selection algorithm to dynamically select better PPG channel in multi-channel PPG measurement system. PPG signal corrupted by motion artifact is effectively denoised by LMK-RLS algorithm and SSA algorithm. After that, peak detection and peak tracking algorithm intelligently select the most suitable peak as the estimated heart rate. We also consider the effect of suddent movement detection algorithm to further tune estimated heart rate. We have tested our algorithm on the dataset used by popular HR estimation frameworks, and our method has shown improved result most of the cases. Even in the highly corrupted subjects like 1, 4 or 10, our framework has shown great accuracy.

References

[1] B. Jonsson, C. Laurent, T. Skau, and L.-G. Lindberg, "A new probe for ankle systolic pressure measurements using photopethysmography," International Angiology, 2004.

[2] P. A. Leonard, J. G. Douglas, N. R. Grubb, D. Clifton, P. S. Addison, and J. N. Watson, "A fully automated algorithm for the determination of respiratory rate from the photoplethysmogram," Journal of Clinical Monitoring and Computing, vol. 20, issue. 1, pp. 33–36, 2006.

[3] L. Nilsson, A. Johansson, and S. Kalman, "Respiration can be monitored by photoplethysmography with high sensitivity and specicity regardless of an aesthesia and ventilator mode," Acta Anaesthesiologica Scandinavica, vol. 49, issue. 8, pp. 1157–1162, 2005.

[4] M. Ram et al., "A novel approach for motion artifact reduction in PPG signals based on AS-LMS adaptive filter," IEEE Trans. Instrum. Meas., vol. 61, no. 5, pp. 1445–1457, May 2012.

[5] X. Sun et al., "Robust heart beat detection from photoplethysmography interlaced with motion artifacts based on empirical mode decomposition," in Proc. IEEE Int. Conf. Biomed. Health Informat., 2012, pp. 775–778.

[6] B. Lee et al., "Improved elimination of motion artifacts from a photoplethysmographic signal using a Kalman smoother with simultaneous accelerometry," Physiol. Meas., vol. 31, no. 12, pp. 1585–1603, 2010.

[7] S. H. Kim, D. W. Ryoo, and C. Bae, "Adaptive noise cancellation using accelerometers for the ppg signal from forehead," in Engineering in Medicine and Biology Society, 2007. EMBS 2007. 29th Annual International Conference of the IEEE., IEEE, 2007, pp. 2564–2567.

[8] M.-Z. Poh, N. C. Swenson, and R. W. Picard, "Motion-tolerant magnetic earring sensor and wireless earpiece for wearable photoplethysmography," IEEE Transactions on Information Technology in Biomedicine, vol. 14, no. 3, pp. 786–794, 2010.

[9] R. Krishnan, B. Natarajan, and S. Warren, "Two-stage approach for detection and reduction of motion artifacts in photoplethysmographic data," IEEE Trans. Biomed. Eng., vol. 57, no. 8, pp. 1867–1876, Aug. 2010.

[10] Pang, Bo, et al. "Advanced EMD method using variance characterization for PPG with motion artifact." Biomedical Circuits and Systems Conference (BioCAS), 2016 IEEE. IEEE, 2016. APA

[11] Raghuram, M., Kosaraju Sivani, and K. Ashoka Reddy. "Use of complex EMD generated noise reference for adaptive reduction of motion artifacts from PPG signals." Electrical, Electronics, and Optimization Techniques (ICEEOT), International Conference on. IEEE, 2016.

[12] Liao, Jia-Ju, et al. "An effective photoplethysmography signal processing system based on EEMD method." VLSI Design, Automation and Test (VLSI-DAT), 2015 International Symposium on. IEEE, 2015.

[13] B. Lee, J. Han, H. J. Baek, J. H. Shin, K. S. Park, and W. J. Yi, "Improved elimination of motion artifacts from a photoplethysmographic signal using a kalman smoother with simultaneous accelerometry," Physiological measurement, vol. 31, no. 12, pp. 1585–1603, 2010.

[14] Schäck, Tim, et al. "A new method for heart rate monitoring during physical exercise using photoplethysmographic signals." Signal Processing Conference (EUSIPCO), 2015 23rd European. IEEE, 2015.

[15] F. Peng et al., "Motion artifact removal from photoplethysmographic sig- nals by combining temporally constrained independent component anal- ysis and adaptive filter," Biomed. Eng. Online, vol. 13:50, no. 1, 2014.

[16] Y. Yan, C. C. Poon, and Y. Zhang, "Reduction of motion artifact in pulse oximetry by smoothed pseudo wigner-ville distribution," Journal of NeuroEngineering and Rehabilitation, vol. 2, no. 1, pp. 1, 2005.

[17] M. Raghuram, K. V. Madhav, E. H. Krishna, and K. A. Reddy, "Evaluation of wavelets for reduction of motion artifacts in photoplethysmographic signals," in Information Sciences Signal Processing and their Applications (ISSPA), 2010 10th International Conference on. IEEE, 2010, pp. 460–463.

[18] X. Sun, P. Yang, Y. Li, Z. Gao, and Y.-T. Zhang, "Robust heart beat detection from photoplethysmography interlaced with motion artifacts based on empirical mode decomposition," in Biomedical and Health Informatics (BHI), 2012 IEEE-EMBS International Conference on. IEEE, 2012, pp. 775–778.

[19] Khan, Emroz, et al. "A robust heart rate monitoring scheme using photoplethysmographic signals corrupted by intense motion artifacts." IEEE Transactions on Biomedical Engineering 63.3 (2016): 550-562.

[20] Z. Zhang, Z. Pi, and B. Liu, "TROIKA: A general framework for heart rate monitoring using wrist-type photoplethysmographic signals during intensive physical exercise," IEEE Transactions on Biomedical Engineering, vol. 62, no. 2, pp. 522–531, 2015.

[21] Z. Zhang, "Photoplethysmography-based heart rate monitoring in physical activities via joint sparse spectrum reconstruction," IEEE Transactions on Biomedical Engineering, vol. 62, no. 8, pp. 1902–1910, 2015.

[22] Chowdhury, Sayeed, et al. "Real Time Robust Heart Rate Estimation from Wrist-type PPG Signals Using Multiple Reference Adaptive Noise Cancellation." IEEE Journal of Biomedical and Health Informatics (2016).

[23] Z. Zhang, "Undergraduate students compete in the IEEE signal processing cup: Part 3," IEEE Signal Processing Magazine, vol. 32, no. 6, 2015.

[24] R.Yousefi et al., "A motion-tolerant adaptive algorithm for wearable photoplethysmographic biosensors,"IEEE J. Biomed. Health Inform.,vol. 18, no. 2, pp. 670–681, 2014.